

Improved electrochemical performance of $\text{Ca}_2\text{Fe}_{1.4}\text{Co}_{0.6}\text{O}_5\text{--Ce}_{0.9}\text{Gd}_{0.1}\text{O}_{1.95}$ composite cathodes for intermediate-temperature solid oxide fuel cells

Qiang Li · Liping Sun · Lihua Huo · Hui Zhao · Jean-Claude Grenier

Received: 1 June 2011 / Revised: 3 July 2011 / Accepted: 12 July 2011 / Published online: 29 July 2011
© Springer-Verlag 2011

Abstract The performance of $\text{Ca}_2\text{Fe}_{1.4}\text{Co}_{0.6}\text{O}_5\text{--Ce}_{0.9}\text{Gd}_{0.1}\text{O}_{1.95}$ (CFC–CGO) composite cathode has been investigated for potential application in intermediate-temperature solid oxide fuel cells (IT-SOFCs). The composite cathodes are prepared and characterized by XRD and SEM, respectively. The electrochemical properties of the composite cathodes are investigated using AC impedance and DC polarization methods from 500 to 700 °C under different oxygen partial pressures. The polarization resistance (R_p) decreases with the increase of CGO content in the composite electrode. The addition of 40 wt.% CGO in CFC results in the lowest R_p of $0.48 \Omega \text{ cm}^2$ at 700 °C in air. Oxygen partial pressure dependence study indicates that the charge-transfer process is the rate limiting step for oxygen reduction reaction. CFC-40CGO composite cathode exhibits the lowest overpotential of about 67 mV at a current density of 85 mA cm^{-2} at 700 °C in air.

Keywords Intermediate-temperature solid oxide fuel cells · Composite cathode · Oxygen reduction reaction

Introduction

Solid oxide fuel cells (SOFCs) are considered as promising next generation electric power source because of their high

efficiency, environmental friendliness, and fuel flexibility. Nowadays, one of the most important research goals is to develop intermediate-temperature solid oxide fuel cells (IT-SOFCs) [1]. IT-SOFCs will solve problems associated with the high operation temperature, such as sealing and thermal degradation. However, the reduced operation temperature leads to decrease in the catalytic activity of the cathode materials for the oxygen reduction reaction [2]. Therefore, the improvement of cathode performance is one of the most important issues for the development of IT-SOFCs.

In the study of alternative cathode materials with nominal formula $\text{A}_2\text{B}_2\text{O}_5$, much attention was focused on their structure and electrochemical properties. As we know, $\text{A}_2\text{B}_2\text{O}_{5+\delta}$ compounds can crystallize in either layered perovskite-type or brownmillerite structures, depending on the value of δ . Layered perovskite-type oxides, $\text{LnBaCo}_2\text{O}_{5+\delta}$ (LnBCO) (Ln = rare earth) have received increasing attention due to their possible application as cathode materials for IT-SOFCs [3–6]. These materials exhibit promising ionic–electronic mixed conductivity and electrocatalytic activity for the oxygen reduction reaction. However, it is reported that the thermal expansion coefficients (TECs) of LnBCO materials vary from 15.8×10^{-6} to $24.3 \times 10^{-6} \text{ K}^{-1}$ in the temperature range of 100–900 °C in air [7]. The large TECs are not compatible with these well-known solid electrolyte materials. In addition, the relatively high cost of cobalt element is another drawback that retards the wide application of LnBCO materials [8].

Recently, a number of oxides with the brownmillerite-type structure have been re-visited, in terms of their high-temperature electrochemical properties. These compounds exhibit relatively high oxygen diffusion ability and suitable TECs [9, 10]. For example, the average TECs of $\text{Ca}_2\text{Fe}_2\text{O}_5$ ceramic is in the range of $(11.3\text{--}13.6) \times 10^{-6} \text{ K}^{-1}$, which is compatible with many solid electrolyte materials [11]. Another study indicated that brownmillerite oxides have

Q. Li · L. Sun · L. Huo · H. Zhao (✉)
Key Laboratory of Functional Inorganic Material Chemistry,
Heilongjiang University, Ministry of Education,
Harbin 150080, People's Republic of China
e-mail: zhaohui98@yahoo.com

J.-C. Grenier
ICMC Bordeaux-CNRS,
87 Avenue du Dr. A. Schweitzer, Université de Bordeaux 1,
33608 Pessac-Cedex, France

potential applications in separating oxygen from air and partial oxidation of light hydrocarbons, due to their high oxygen permeability [12, 13]. The electrochemical properties of $\text{Ca}_2\text{Fe}_{2-x}\text{Co}_x\text{O}_5$ (CFC) cathode materials for IT-SOFCs were recently studied in our group [14]. These materials exhibited reduced polarization resistance and compatible chemical stability with CGO electrolyte, which implies that $\text{Ca}_2\text{Fe}_{2-x}\text{Co}_x\text{O}_5$ is likely to be new cathode material for IT-SOFCs.

It is generally agreed that composite electrodes, which typically consist electronic conducting materials and ionic conducting materials, exhibit improved electrochemical performance than those single-phase ones. This is due to the enlargement of the electrochemical active area, i.e., the triple phase boundary (TPB) in the composite electrode [15]. Several composite materials, such as $\text{La}_{0.8}\text{Sr}_{0.2}\text{MnO}_3\text{-Ce}_{0.9}\text{Gd}_{0.1}\text{O}_{1.95}$ (LSM–CGO), $\text{La}_{0.6}\text{Sr}_{0.4}\text{Co}_{0.2}\text{Fe}_{0.8}\text{O}_3\text{-Ce}_{0.9}\text{Gd}_{0.1}\text{O}_{1.95}$ (LSCF–CGO), and $\text{Sm}_{0.5}\text{Sr}_{0.5}\text{CoO}_3\text{-Sm}_{0.2}\text{Ce}_{0.8}\text{O}_{1.9}$ (SSC–SDC) [16–18], have been extensively studied and show attractive electrochemical properties.

In order to further optimize the electrochemical performance of CFC material, $\text{Ca}_2\text{Fe}_{1.4}\text{Co}_{0.6}\text{O}_5\text{-Ce}_{0.9}\text{Gd}_{0.1}\text{O}_{1.95}$ (CFC–CGO) composite cathode was prepared. $\text{Ca}_2\text{Fe}_{1.4}\text{Co}_{0.6}\text{O}_5$ exhibits the highest electrical conductivity (80 s cm^{-1} at $800 \text{ }^\circ\text{C}$ in air) among the series $\text{Ca}_2\text{Fe}_{2-x}\text{Co}_x\text{O}_5$ material which is benefit to extend the active oxygen reduction site from the TPB to the whole exposed cathode surface. The chemical compatibility, cathode properties, and kinetics of oxygen reduction reaction were investigated and analyzed in detail.

Experimental

$\text{Ca}_2\text{Fe}_{1.4}\text{Co}_{0.6}\text{O}_5$ (CFC) powder was prepared via the solid-state reaction. Stoichiometric amount of CaCO_3 (99.99%), Fe_2O_3 (99.99%), and Co_3O_4 (99.99%) were mixed and grounded in an agate mortar, then calcined in air at $1,100 \text{ }^\circ\text{C}$ for 24 h. $\text{Ce}_{0.9}\text{Gd}_{0.1}\text{O}_{1.95}$ (CGO) powder was prepared according to ref. [19]. The CGO powders were uniaxially pressed at 220 MPa and then sintered at $1,400 \text{ }^\circ\text{C}$ for 10 h to form a dense electrolyte pellet. The pellet was about 1 mm in thickness and 15 mm in diameter.

The CFC powders were mixed with different amount of CGO powders (0–50 wt.%) to form composite material (denoted here by “CFC- x CGO” $x=0\text{--}50$). The CFC- x CGO powders were first mixed with terpineol to form the slurry, and subsequently painted on one side of the CGO electrolyte to form a working electrode (WE) with area of 0.5 cm^2 . Platinum paste was painted on the other side of the CGO pellet in symmetric configuration, as the counter electrode (CE). A Pt wire with diameter of 0.1 mm was

used as reference electrode (RE). This Pt wire was welded on the working-electrode side of the CGO electrolyte with Pt paste, to form a point contact (less than 0.5 mm in diameter) on the edge of CGO electrolyte. The RE was normally placed 5 mm away from the WE, ensuring that this distance was more than three times the thickness of the electrolyte.

The structure and phase purity of the materials were investigated by X-ray powder diffraction on a Bruker D8-Advance diffractometer Cu K_α radiation. The morphology and microstructure of the sintering electrodes were examined with Hitachi S-4700 FEG-SEM (field emission gun-scanning electron microscope). The electrochemical impedance spectra (EIS) were recorded in the frequency range 0.1 Hz–1 MHz using Autolab PGStat30, and EIS fitting analysis was performed with the Zview software. The measurements were performed at equilibrium potential as a function of temperature (500–700 $^\circ\text{C}$) and oxygen partial pressure.

The DC polarization experiments were performed by the chronoamperometry method [20], which involved a potential step followed by recording the current density as a function of time. The cathode overpotential was calculated according to the following equation:

$$\eta_{\text{WE}} = \Delta U_{\text{WR}} - iR_{\text{el}}$$

where η_{WE} represents the cathode overpotential, ΔU_{WR} is the applied voltage between working electrode and reference electrode, i is the current flowing through the test cell, and R_{el} is the resistance of the electrolyte obtained from the impedance spectrum.

Results and discussions

Chemical stability of the cathode material

It is known that the interfacial reaction between cathode and electrolyte materials has dramatic effect on the performance of SOFCs [21]. It is necessary to study the chemical stability of CFC with CGO at high temperature. The sample was prepared by mixing thoroughly CFC with CGO powers in a 1:1 weigh ratio, and then heat-treated at $1,200 \text{ }^\circ\text{C}$ for 12 h in air. The phase evolution and possible reaction was checked by XRD. Figure 1 shows the XRD pattern of heat-treated mixture. For comparison, the XRD patterns of CFC and CGO were also presented. It was observed that CGO and CFC remained their structure unchanged; no new diffraction patterns were detected except those of CFC and CGO. This result indicates that CFC has no reaction with CGO electrolyte. Compared to the reported perovskite cobaltic oxide (such as $\text{Ba}_{0.5}\text{Sr}_{0.5}\text{Fe}_y\text{Co}_{1-y}\text{O}_3$) [22], the brownmillerite $\text{Ca}_2\text{Fe}_{2-x}\text{Co}_x\text{O}_5$ oxide exhibits much

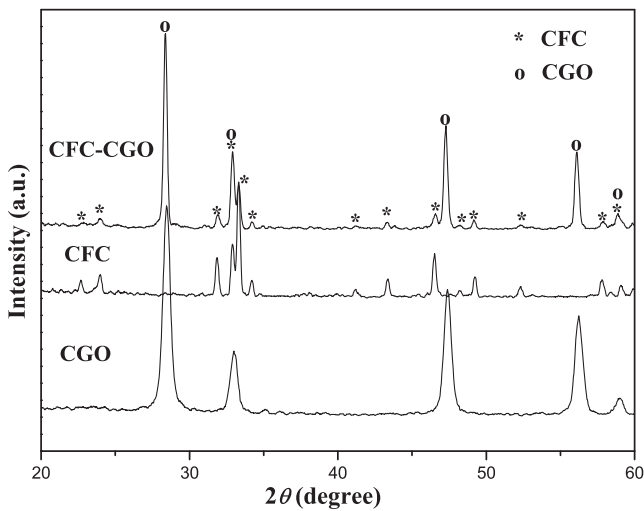


Fig. 1 XRD patterns of CFC, CGO, and CFC–CGO mixture after 1,200 °C for 12 h in air

higher thermal and chemical stability, which is advantageous when the SOFCs system has to work for a long time.

Electrochemical measurements of the cathode material

Figure 2 shows the typical impedance spectra of the CFC-40CGO composite cathode on CGO electrolyte after sintered at different temperatures for 4 h and then measured at 700 °C in air. There are at least two consecutive arcs presented when the sintering temperature is 900 and 1,100 °C. However, only one arc presents when the sintering temperature is 1,000 °C. Here, the intercepts of the impedance arc with the real axis at high frequencies correspond to the resistance of the electrolyte and lead wires, whereas the overall size of the arcs is attributed to cathode polarization resistance (R_p) of the CFC-40CGO composite electrode. It is observed that R_p was relatively high when the sintering temperature was low (900 °C). When the sintering temperature was 1,000 °C, R_p reduced to the lowest value. R_p increased again when the sintering temperature was 1,100 °C. As we know, the sintering temperature has dramatic effect on the electrode microstructure, which in turn will influence the electrode properties. Therefore, the microstructure evolution of the CFC-40CGO composite cathode under different sintering temperatures was further studied by SEM. Clearly from Fig. 3a, it is observed that electrode particles formed poor contact with each other when the sintering temperature was 900 °C. After being sintered at 1,000 °C, a microstructure with moderate porosity and well-necked particles was formed. The average particle size is about 200 nm, and the thickness of the electrode is about 40 μm (Fig. 3b, d). When the electrode was sintered at 1,100 °C for 4 h, the diameter of CFC particles increases dramatically, and the particles are partially aggregated, as that shown in Fig. 3c. In this case,

the increase of polarization resistance might be due to further growth and agglomeration of the particles, which decreases the cathode porosity and retards the gas diffusion. The activated reaction sites in the CFC–CGO cathode also decrease. Consequently, the electrode performance is weakened, and the cathode exhibits high polarization resistance. The similar over-sintering effect has been observed before in the other cathode materials [23]. Therefore, 1,000 °C for 4 h is the best sintering condition for CFC–CGO electrode to obtain optimum microstructure.

The effects of CGO content on the polarization resistance were further studied. Figure 4 shows the polarization resistance (R_p) versus measurement temperature for composite cathodes. The R_p of pure CFC cathode is 1.05 Ω cm² at 700 °C in air. R_p decreases steadily as the CGO content increases from 0 to 40 wt.%. The lowest R_p of 0.48 Ω cm² is obtained at 700 °C when CGO content is 40 wt.%. However, when CGO content increases to 50 wt.%, cathode polarization resistance increases again. This phenomenon can be explained by ambipolar resistivity model of porous composite cathode developed by Dusastre et al. [24]. The decrease in R_p with the addition of CGO could be attributed to the high ionic conductivity of CeO₂-based oxides [25], which functions effectively as an oxygen conduction path, and greatly extends the electrochemical-activated reaction sites from the electrode/electrolyte interface to the bulk of the CFC electrode, which results in a decrease in the polarization resistance. At very high CGO content, the electron-conducting path within CFC particles may be interrupted, which results in the increase of polarization resistance. In addition, the presence of non-continuous electron-conducting phase in CFC–CGO composite cathode leads to high-ohmic resistance and contact resistance between the cathode and electrolyte substrate. Therefore,

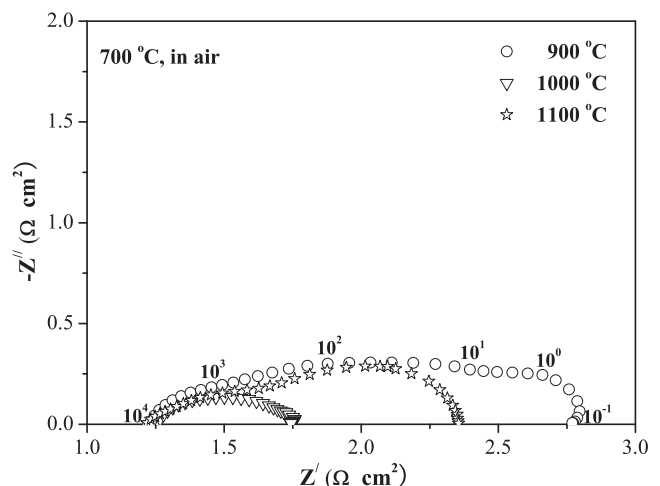
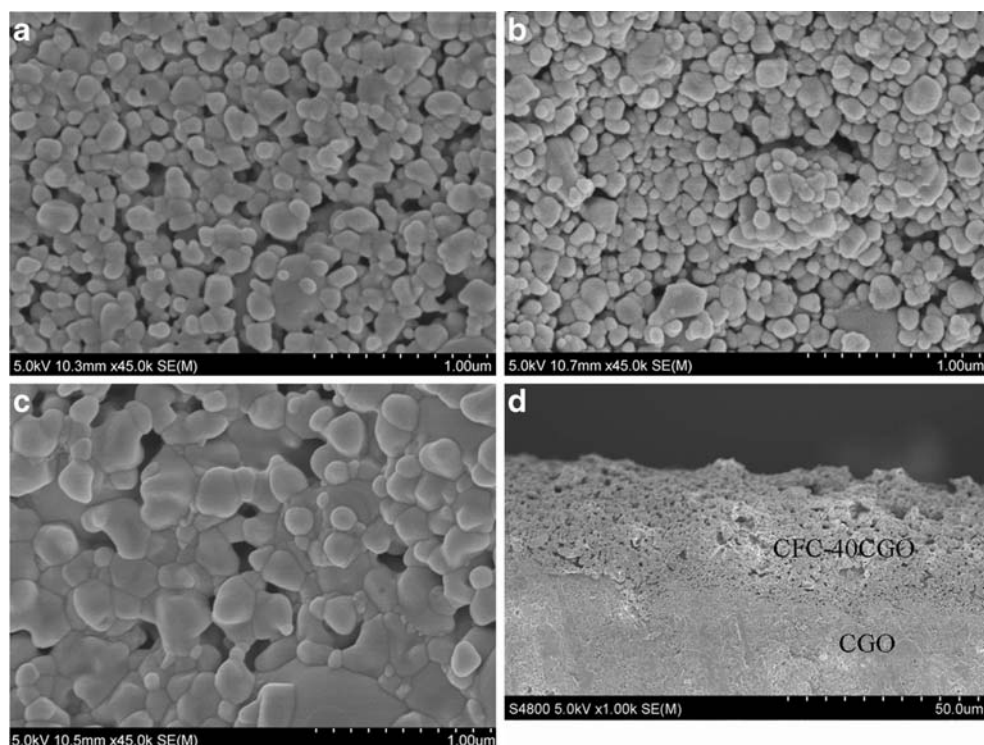


Fig. 2 Impedance spectra of the CFC-40CGO composite cathode sintering at different temperatures and then measured at 700 °C in air

Fig. 3 SEM micrographs of the CFC-40CGO composite cathode sintered at 900 (a); 1,000 (b); 1,100 °C (c); and the cross-section micrograph of the test cell sintered at 1,000 °C (d)



the optimal CGO content to achieve the lowest cathode polarization resistance was 40 wt.% in this study. This result is quite similar to the reported composite cathodes, such as LSM–CGO and LSCF–CGO [16, 26]. Therefore, in the below experiments, only the optimum composite electrodes (with 40 wt.% CGO and sintered at 1,000 °C for 4 h) are investigated.

The temperature dependence of polarization resistances R_p with various CGO compositions is presented in Fig. 5.

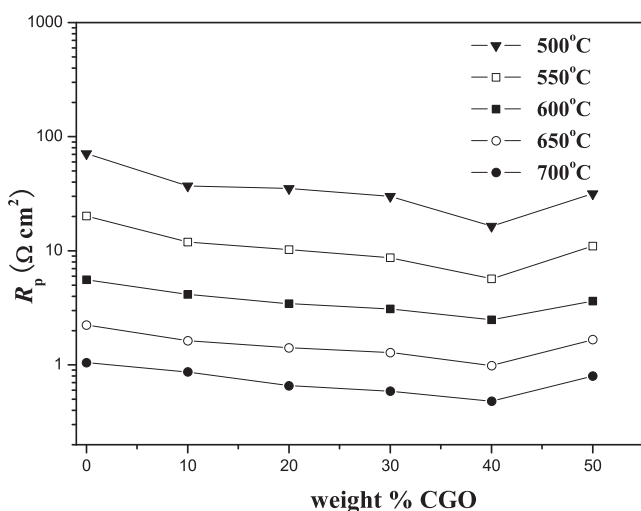


Fig. 4 Polarization resistance R_p of CFC–CGO composite cathodes (sintered at 1,000 °C) as a function of CGO content, measured at 500–700 °C in air

From the slope of the curves, the activation energy can be calculated. The slopes of $\log R_p$ vs. $1/T$ are nearly the same for all CFC–CGO compositions, yielding activation energy from 1.14 to 1.28 eV. These values are close to that of pure CFC cathode (1.39 eV) [14]. This indicates that the CGO addition does not change the rate limiting mechanism of the cathode reaction process.

To clarify the oxygen reduction reaction mechanism of the composite electrode, impedance measurements were performed as a function of oxygen partial pressure. Figure 6 shows the dependence of polarization resistance (R_p) of the CFC-40CGO/CGO test cell on oxygen partial pressure (P_{O_2}) at different temperatures. It is observed that the polarization resistance decreases dramatically with the increase of oxygen partial pressure. Generally, R_p varies with the oxygen partial pressure according to the following equation:

$$R_p = R_p^0 (P_{O_2})^{-n}$$

$n = 1$, $O_2(g) \rightleftharpoons O_{2,ads}$.
 (molecular oxygen is absorbed on the electrode surface)
 $n = 1/2$, $O_{2,ads} \rightleftharpoons 2O_{ads}$.
 (oxygen surface adsorption, dissociation and surface diffusion)
 $n = 1/4$, $O_{ads} + 2e^- + V_{O}^{\bullet} \rightleftharpoons O_O^x$.
 (charge – transfer process)

It is known that the value of n could give useful information about the type of species involved in the electrode reactions [27, 28]. The $P_{O_2}^{1/4}$ relationship was considered as the contribution of the charge-transfer process

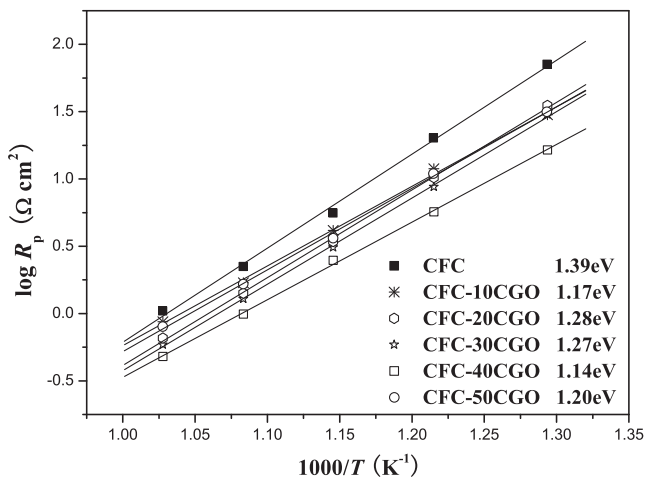


Fig. 5 Temperature dependence of the R_p for CFC and CFC–CGO composite cathodes

on the electrode, which was observed before for Nd_2NiO_4 cathode [29]. Our results indicated that the n value is 0.23 ± 0.02 at 700°C , 0.24 ± 0.02 at 600°C , and 0.24 ± 0.01 at 500°C , respectively, which is quite near the value of 0.25 ($n=1/4$). This result indicates that the charge-transfer process is the major rate limiting step for CFC-40CGO composite cathode in the whole range of measurement oxygen partial pressure. The same conclusion has been drawn in our previous study of pure $\text{Ca}_2\text{Fe}_{2-x}\text{Co}_x\text{O}_5$ cathode material [14]. This implies that the addition of CGO does not change the reaction limiting step of the composite electrode.

Cathode overpotential is an important factor representing the electrode performance. Figure 7 shows the cathodic polarization curve of CFC-40CGO composite cathode measured at various temperatures in air. At low overpotential (less than 20 mV), we can expect a linear expression

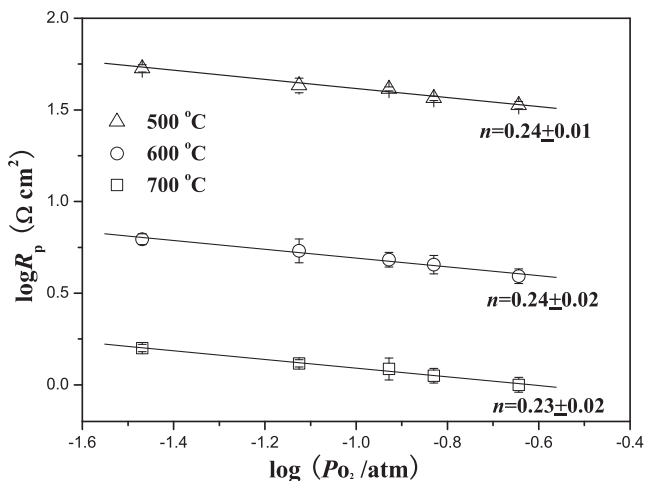


Fig. 6 Dependence of R_p on oxygen partial pressure for CFC-40CGO composite cathode at 500, 600, and 700°C

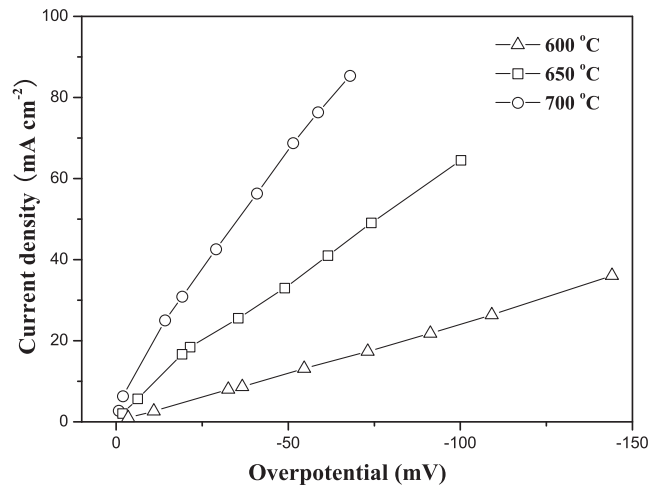


Fig. 7 Cathodic polarization curves for CFC-40CGO composite cathode obtained at various temperatures in air

[30], $i = i_0 ZF\eta/RT$, where i is the current density, i_0 the exchange current density, η the overpotential, F is the Faraday's constant, and R is the universal gas constant. From the inverse of the derivative of i against η , we can obtain the polarization resistance. The value obtained at 700°C in air was $0.50 \Omega \text{ cm}^2$, which was in agreement with the result obtained from impedance measurement. It is also observed from Fig. 7 that the current density (for a fixed overpotential value) increases with temperature. The lowest polarization overpotential, 67 mV, was measured for CFC-40CGO composite cathode at a current density of 85 mA cm^{-2} at 700°C in air. This value is lower than that of the reported LSM-CGO composite cathode [16]. As we expected, the polarization overpotential can be reduced dramatically by forming a composite cathode with high electronic and ionic-conducting materials, and that CFC–CGO composite materials can be considered as possible cathodes for IT-SOFCs. Further work will be done to optimize the microstructure and to improve the catalytic properties of the electrode.

Conclusions

1. The CFC–CGO composite cathode forms good contact with CGO electrolyte after sintering at $1,000^\circ\text{C}$ for 4 h.
2. Impedance analysis and oxygen partial pressure dependence study indicate that charge-transfer process is the rate limiting step for oxygen reduction reaction. The reaction rate limiting step does not change with the addition of CGO.
3. The lowest polarization resistance obtained at 700°C in air is $0.48 \Omega \text{ cm}^2$ for the CFC-40CGO composite cathode, and the lowest overpotential is 67 mV under a current density of 85 mA cm^{-2} .

Acknowledgments The project was supported by national Natural Science Foundation of China (51072048), Heilongjiang Educational Department (GZ09A204, 1152G027, 11531274), Heilongjiang Province Postdoctoral Foundation (LBH-Z09019), China Postdoctoral Science Foundation (20100471116).

References

1. Brett D, Atkinson A, Brandon NP, Skinner SJ (2008) *Chem Soc Rev* 37:1568–1578
2. Sun CW, Hui R, Roller J (2010) *J Solid State Electrochem* 14:1125–1144
3. Lin B, Dong YC, Yan RQ, Zhang SQ, Hu MJ, Zhou Y, Meng GY (2009) *J Power Sourc* 186:446–449
4. Zhao L, He BB, Lin B, Ding HP, Wang SL, Ling YH, Peng RR, Meng GY, Liu XQ (2009) *J Power Sourc* 194:835–837
5. Tarancón A, Martínez JP, López DM, Morata A, Morales JCR, Núñez P (2008) *Solid State Ionics* 179:2372–2378
6. Gu HT, Chen H, Gao L, Zheng YF, Zhu XF, Guo LC (2009) *Int J Hydrogen Energ* 34:2416–2420
7. Kim JH, Manthiram A (2008) *J Electrochem Soc* 155:B385–B390
8. Kim JH, Kim Y, Connor PA, Irvine JTS, Bae J, Zhou WZ (2009) *J Power Sourc* 194:704–711
9. Sharma N, Shaju KM, Rao GVS, Chowdari BVR (2004) *Electrochim Acta* 49:1035–1043
10. Calle C, Alonso JA, Aguadero A, Fernández-Díaz MT (2009) *Dalton Trans* 21:4104–4114
11. Shaula AL, Pivak YV, Waerenborgh JC, Gaczyński P, Yaremchenko AA, Kharton VV (2006) *Solid State Ionics* 177:2923–2930
12. Liu YT, Tan XY, Li K (2006) *Catal Rev* 48:145–198
13. Yang WS, Wang HH, Zhu XF, Lin LW (2005) *Top Catal* 35:155–167
14. Li Q, Sun LP, Huo LH, Zhao H, Grenier JC (2010) *Int J Hydrogen Energ* 35:9151–9157
15. Wu ZL, Liu ML (1996) *Solid State Ionics* 93:65–84
16. Murray EP, Barnett SA (2001) *Solid State Ionics* 143:265–273
17. Leng YL, Chan SH, Liu QL (2008) *Int J Hydrogen Energ* 33:3808–3817
18. Sun WP, Yan LT, Lin B, Zhang SQ, Liu W (2010) *J Power Sourc* 195:3155–3158
19. Zha SW, Moore A, Abernathy H, Liu ML (2004) *J Electrochem Soc* 151:A1128–A1133
20. Espurol A, Brandon N, Bonanos N, Kilner J, Mogensen M (2002) *Proceedings of the Fifth European Solid Oxide Fuel Cell Forum*, U. Bossel, Oberrohrdorf, Switzerland, pp 225–232
21. Letilly M, Le Gal La Salle A, Lachgar A, Joubert O (2010) *J Power Sourc* 195:4779–4784
22. Li SY, Lü Z, Wei B, Huang XQ, Miao JP, Liu ZG, Su WH (2008) *J Alloy Comp* 448:116–121
23. Li Q, Zhao H, Huo LH, Sun LP, Cheng XL, Grenier JC (2007) *Electrochem Commun* 9:1508–1512
24. Dusastre V, Kilner JA (1999) *Solid State Ionics* 126:163–174
25. Mogensen M, Sammes NM, Tompsett GA (2000) *Solid State Ionics* 129:63–94
26. Qiang F, Sun KN, Zhang NQ, Zhu XD, Le SR, Zhou DR (2007) *J Power Sourc* 168:338–345
27. Takeda Y, Kanno R, Noda M, Yamamoto O (1987) *J Electrochem Soc* 134:A2656–A2661
28. Sicbeit E, Hammouche A, Kleitz M (1995) *Electrochim Acta* 40:1741–1753
29. Mauvy F, Bassat JM, Boehm E, Manaud JP, Dordor P, Grenier JC (2003) *Solid State Ionics* 158:17–28
30. Steele BCH (1995) *Solid State Ionics* 75:157–165